Available online at www.sciencedirect.com
ScienceDirect
Thin Solid Films 516 (2008) 6771–6774
www.elsevier.com/locate/tsf

Innovative design of amorphous/crystalline silicon heterojunction solar cell

M. Tucci [a,*], L. Serenelli [a], E. Salza [a], M. Rattè [a], S. De Iuliis [b], L.J. Geerligs [b], D. Caputo [c], A. Nascetti [c], G. de Cesare [c]

[a] ENEA Research Center Casaccia Via Anguillarese 301, 00123 Roma, Italy
[b] ECN Solar Energy, P.O. Box 1, 1755 ZG Petten, The Netherlands
[c] Department of Electronic Engineering University of Rome "La Sapienza", via Eudossiana, 18, 00184 Roma, Italy

Available online 24 January 2008

Abstract

In this work we show how the heterostructure technology can have a chance in the challenge of interdigitated back contact solar cell. We present an innovative rear junction, backside contact design in which both the emitter and the back surface field are formed by amorphous/crystalline silicon heterostructure, and the grid-less front surface is passivated by a double layer of amorphous silicon and silicon nitride, which also provides a good anti-reflection coating. The technological processes are performed at temperature below 300 °C with the aid of one metallic mask to create the interdigitated pattern. The initials results, on a p-type monocrystalline silicon wafer; are really promising, a V_{oc} of 687 mV has been reached. We show that the uniformity of the deposited amorphous silicon layers is not influenced by the mask-assisted deposition process and that the alignment is feasible. On the other hand several technological aspects that strongly limit the fill factor (50%) and the short circuit current density (30 mA/cm^2) have to be optimized.

Keywords: Heterostructure; Amorphous; Crystalline

1. Introduction

Recently, there has been renewed industrial interest in high efficiency silicon solar cells. This interest is motivated by the large leveraging effect that higher cell efficiency has in reducing overall photovoltaic module and system costs [1–3]. Top performing production cells include SunPower's A-300 cell [4], and Sanyo's HIT cell [5]; both technologies have demonstrated almost 22% as cell efficiency, starting from n-type monocrystalline silicon wafers. The back contact technology allows improvement of the module active area fraction as both contacts are on the rear, and the solar cells can be placed closer together in the module because there is no need for a space between the cells for interconnect tabs [6]. On the other hand A-300 cell technology includes three high temperature steps; moreover SunPower has identified recombination at the contacts as a major limiting factor to obtaining even higher efficiency, individuating the heterojunction as a possible way of improvement [7]. Sanyo's HIT structure enables an excellent surface passivation of c-Si surface defects, including the contacts, by high-quality intrinsic amorphous silicon (a-Si:H) layers. Thus results in high efficiency, especially a high V_{oc}: almost 730 mV has been reached [8,9]. The low-temperature processes (<200 °C) and the symmetrical structure of HIT cells can suppress both thermal and mechanical stress during its production process and results in an advantage for thinner wafers. The temperature coefficient of HIT cells is better than conventional c-Si solar cells and results in a higher output power at high temperatures [10]. One of the problems of the amorphous/crystalline silicon (a-Si:H/c-Si) heterostructure is a loss of quantum efficiency in the blue region of the solar spectrum due to the absorption of the front side a-Si:H window layer, furthermore if the cell is based on p-type doped c-Si the blue response is also worse due to the difficulty to increase the band-gap of the n-type amorphous layer. Additionally, the front side a-Si:H has to be covered with a thin conductive oxide which results in absorption loss in the infrared region.

To combine the strength of both technologies described above, we present an innovative design of the solar cell in which both the emitter and the back surface field are formed by a-Si:H/c-Si heterostructure, and the grid-less front surface is passivated

* Corresponding author. Tel.: +390630484095; fax: +390630486405.
E-mail address: mario.tucci@casaccia.enea.it (M. Tucci).

0040-6090/$ - see front matter © 2007 Elsevier B.V. All rights reserved.
doi:10.1016/j.tsf.2007.12.019

by a double layer of amorphous silicon and silicon nitride (a-Si:H/SiN_x), which also provides a good anti-reflection coating. We have named this device: BEHIND cell (Back Enhanced Heterostructure with INterDigitated contacts cell). In this paper we present the preliminary results on untextured p-type monocrystalline silicon wafers, we show that the uniformity of the deposited a-Si:H layers is not influenced by the mask-assisted deposition process and that the alignment is feasible. Finally we analyze these results by individuating way of improvements.

2. Experimental

Since the approach to solar cell with rear side contacts presents severe difficulties, it is preferable, in the first set up of the process, the use of good quality substrates to reduce the defect density at the most critical interface as well as ensure a sufficient diffusion length. So to fabricate our BEHIND cells we have chosen: 4 in. diameter, <100> oriented, 250 μm thick, 0.5 Ω cm p-type doped, and one side polished FZ silicon wafers. In particular the polished side has been used as the back side of the device. The wafer, after a RCA cleaning and HF dip, has been introduced in a 13.56 MHz direct Plasma Enhanced Chemical Vapor Deposition (PECVD) system to deposit a 5 nm thick intrinsic a-Si:H layer and a 15 nm thick n-type doped a-Si:H layer on the whole polished side at the following conditions:

(1) *i a-Si:H layer*: RF power density=28 mW/cm^2; T=300 °C; P=300 mTorr; Gas flow=40 sccm SiH_4.
(2) *n a-Si:H layer*: RF power density=28 mW/cm^2; T=300 °C; P=300 mTorr; Gas flows:10 sccm PH_3/SiH_4 5%; 40 sccm SiH_4.

To reduce interface damages between the two amorphous films we have grown intrinsic and n-doped layers in the same chamber avoiding interruption of glow discharge. Then the wafer has been turned over and after a native oxide removal in a 1% HF wet bath, we have deposited the (a-Si:H/SiN_x) double layer at the following conditions:

(3) *i a-Si:H layer*: RF power density=28 mW/cm^2, T=250 °C, P=750 mTorr, Gas flow=120 sccm of 5% SiH_4 diluted in Ar.
(4) *SiN_x layer*: RF power density=200 mW/cm^2, T=250 °C, P=750 mTorr, 1.66 as NH_3/SiH_4 gas flows ratio.

Choosing thicknesses of 5 nm and 70 nm for a-Si:H and SiN_x respectively, we have also ensured anti-reflection against sun spectrum. We have adopted the amorphous/silicon nitride double layer on the base of previous experience, since it has demonstrated to perform better passivation of crystalline silicon surface with respect to the SiN_x alone [11].

For the p-type back side contact a particular mask has been fabricated from a 100 μm thick Molybdenum foil, on which a comb shape grid has been opened focusing a Nd-YAG laser at a wavelength of 1064 nm. From the geometrical point of view we have dimensioned the distance between two adjacent fingers of the interdigitated combs supposing a diffusion length of minority photogenerated carriers in the order of 400 μm. This mask has been fixed by a particular holder on the n-type a-Si:H covered crystalline wafer, then a dry etching procedure using NF_3 gas has been performed to remove the n-type a-Si:H portion not covered by the mask, using the following conditions on the base of previous experiences [12]:

(5) RF power density=400 mW/cm^2; T=25 °C; P=50 mTorr, Gas flow=48 sccm NF_3.

At the end of the etching process the metallic mask has not been removed and the process trough the mask has been performed in the same PECVD system. To ensure an isolation between the n a-Si:H edges and the p a-Si:H before this last layer we deposit a very thin intrinsic buffer layer of about 5 nm in the conditions above reported at point (1). Then the p-type, 15 nm, has been deposited through the mask in the following conditions:

(6) *p a-Si:H layer*: RF power density=28 mW/cm^2; T=300 °C; P=300 mTorr; Gas flows: 6 sccm of B_2H_6; 40 sccm SiH_4.

Keeping the metallic mask still held on the sample we have evaporated a 2 μm of Al on the p-type a-Si:H. Then we have rotated of 180 degrees the mask in the holder and evaporated a 2 μm of Ag on the n-type a-Si:H layer. The total area of the device is 6.25 cm^2. A schematic view of the entire process is shown in Fig. 1. At this stage the BEHIND cell has been characterized in terms of current voltage (I–V), both in dark and AM1.5G conditions, reflectance and Quantum Efficiency (IQE internal quantum efficiency; EQE external quantum efficiency).

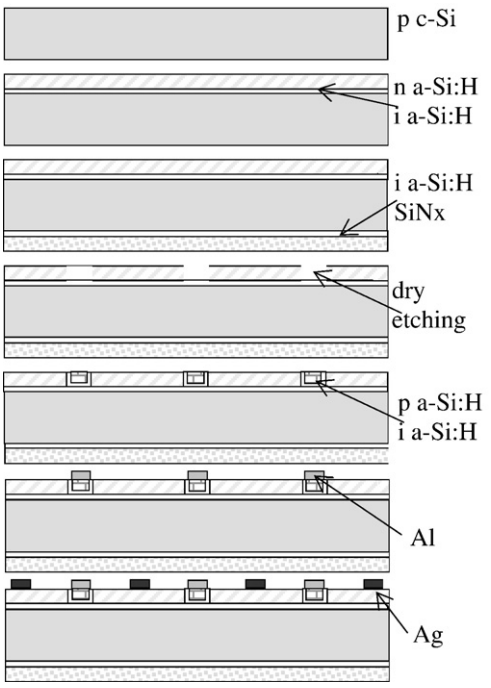

Fig. 1. Schematic view of the fabrication process.

As we will discuss in the next section, to reduce the series resistance, by a Q-switched Nd-YAG laser we have irradiate the Al contact following the comb pattern with a PC controlled XY stage able to move the substrate at 10 mm/s under the beam. On the base of previous work [13] we used the following laser settings: wavelength at 1064 nm, mode TEM_{00}, power 320 mW, repetition rate 1 KHz.

3. Results and discussion

3.1. Technological issues

Every time someone thinks about a solar cell with both rear side contacts quickly realizes that the needed step numbers and mask levels will be not appealing for the PV manufacturing. Therefore each new process in this kind of field should be simplified as much as possible. Moreover looking forward at thinner crystalline silicon wafers low thermal budget processes should be preferred. Our approach on BEHIND cell fabrication has been focused on both issues. The maximum temperature of the entire process does not exceed 300 °C and only one metal mask has been used. Particular care has been taken to the etching time to avoid total removal of the intrinsic buffer layer, causing damages and fluorine radicals contaminations at the silicon surface. After trial and error procedure we have estimated 30 s as sufficient time to etch about 15 nm that corresponds to the n-layer thickness. Moreover when the dry etching is performed through a thick metallic mask leaned on the surface of sample, proximity effect occurs along the edges of the opened pattern that limits the pattern transfer underneath as well as the expected etch rate, even if an anisotropic etching is adopted. The conformal deposition of the intrinsic buffer layer before the p-type one has been useful to reduce unwanted shunt effects between the two a-Si:H doped layers. This has been confirmed by the high open circuit voltage (V_{oc}) measured under the AM1.5G: 687 mV, as reported in Fig. 2.

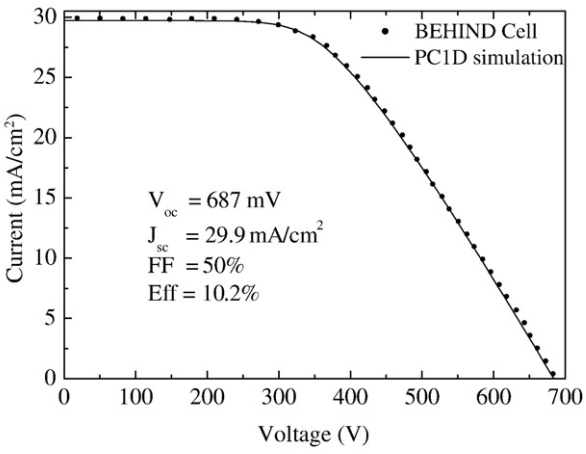

Fig. 2. *I–V* measurements and photovoltaic parameters under AM1.5G condition after laser treatment, experimental data (symbols) and PC1D simulations (lines).

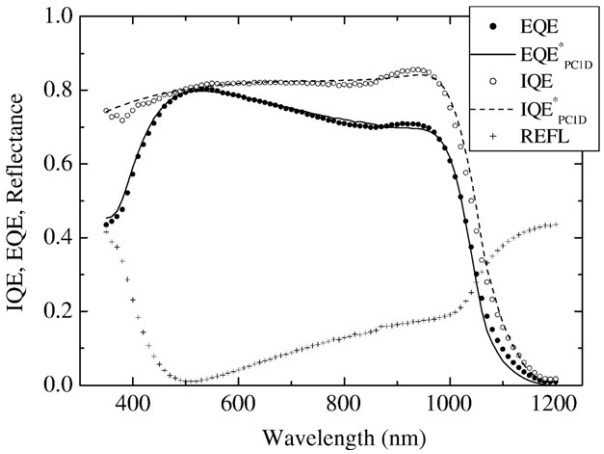

Fig. 3. IQE, EQE, Reflectance of the cell, experimental data (symbols) and PC1D simulation (line).

3.2. Cell characteristics

The 687 mV as V_{oc} value confirms that the uniformity of the deposited amorphous silicon layers is not influenced by the mask-assisted deposition process and that the alignment is feasible. The absence of shadowing by a front metal grid should reflect in high short circuit value (J_{sc}), with respect to the conventionally front grid contacted solar cells. But, as first result, J_{sc} has not exceeded 30 mA/cm^2, as reported in Fig. 2, and also confirmed by integrating the EQE over the sun spectrum, (see Fig. 3). This low value in J_{sc} is due to both optical and recombination losses. Indeed we have not used a crystalline textured surface and the anti-reflection provided by a-Si:H/SiN_x is still affected by a-Si:H absorption in the high energy photons of the sun spectrum. This, in principle, can be reduced increasing the gap of the a-Si:H with hydrogen dilution during the thin film growth. On the other hand a-Si:H is useful to reduce the surface recombination on both crystalline silicon surfaces [11], as needed to achieve high carrier diffusion length. This parameter has been evaluated by the EQE measurements using in particular a spot size of 35 mm^2 of monochromatic light greater than the finger dimensions of the interdigitated contacts. Therefore the effect of different depletion depth of region closer to both n-type emitter and the p-type contact has been averaged. Moreover the evidence of a swelling in the EQE as well as in the IQE data in the spectral region, between 900 nm and 950 nm, ensures a good charge photogeneration also in the depletion region, confirming the wide extension of emitter region. Indeed, at the end of fabrication process, the current of the cell has been completely dominated by the very high series resistance. To verify these arguments we have performed a laser treatment over the Al comb, knowing that this treatment is able to promote, in the right conditions, Al and Boron (being within the p-type a-Si:H material) diffusion into the crystalline base, producing a less resistive contact, even if in a narrow region. Therefore the *I–V* curve collected under AM1.5G at room temperature, reported in the Fig. 2, refers to the cell measured after laser treatment.

3.3. Simulations

We have performed a simulation by PC1D [14] to exploring the photocurrent limiting factors. We have modeled our BEHIND cell simplifying it in one dimensional crystalline silicon based solar cell, having back side emitter, and taking into account the reflectance profile of the front side as measured on the cell and reported in Fig. 3. The n-type emitter has been dimensioned by $5\cdot10^{17}$ cm^{-3} uniformly doped thin film having a-Si:H absorption, $\mu\tau=1\cdot10^{-9}$ cm^2/V and $E_{gap}=1.65$ eV, as expected for n-type doped a-Si:H. The simplified model of the cell has been in agreement with the experimental EQE as well as the IQE data, except for the region of higher energy photons, since the simulation does not account for the passivation/anti-reflection coating absorption. To get better, at the end of EQE calculation, the data have been reduced, at each wavelength, by the a-Si:H thin layer absorption as follows:

$$EQE^{*}_{PCID}(\lambda) = EQE_{PCID}(\lambda)\cdot e^{-\alpha_{a\text{-}Si:H}(\lambda)\cdot d} \quad (1)$$

where: $\alpha_{a\text{-}Si:H(\lambda)}$ is the a-Si:H absorption coefficient and $EQE_{PC1D(\lambda)}$ is the EQE data as calculated by PC1D. By choosing a thickness $d=2$ nm it is possible to obtain the best fit of the EQE data in the spectrum region of higher energy photons, as reported in Fig. 3 as continuous and dashed line for EQE and IQE data respectively. From the fitting procedure we have deduced a front surface recombination S_f of 80 cm/s and a diffusion length L_d of 500 μm and the internal reflectance from the back side R_b is about 50%, while the recombination velocity at the back side is less relevant due to the $\mu\tau$ of the a-Si:H. Starting from the parameter values fixed to obtain the data fit, it is possible to simulate how to reach highest IQE values. To this aim, we have found that S_n of 10 cm/s and a L_n of 1 mm or a wafer thickness reduction down to 170 μm are needed as well as the back reflectance has to be improved. To fit the experimental data of the lighted J–V curve by the PC1D modeling an external high series resistance has been used (continuous line in Fig. 2).

3.4. Improvements

While a lower S_n and longer L_n can be reached having more care in substrate preparation, as demonstrated by the same group in other work [15], actually the most serious problem of the BEHIND cell is the high series resistance that strongly reduces the fill factor. This problem mainly arises from the p-type c-Si/i a-Si:H/p-type a-Si:H contact. Indeed, as detailed elsewhere [16], due to the relevant band offset between the two valence band of p-type c-Si and p-type a-Si:H, the way to extract charge is a tunneling mechanism that can be obtained reducing the thicknesses of p-type and of the intrinsic amorphous layers and introducing an alternative method to increase the conductivity of the p-type a-Si:H layer. Maybe, in our case, these thicknesses have been thicker than expected, since the necessity to avoid shunts between the two amorphous doped layers has wrongly induced to deposit thicker buffer layers. To reduce this value, a large number of fingers should be introduced per square centimeter and a treatment to increase the n-type layer conductivity, forming a thin CrSi layer on it, can be really useful of the n-type amorphous emitter [16].

4. Conclusion

In this paper we have shown the BEHIND cell as an innovative design of the a-Si:H/c-Si heterostructure solar cell. It is a back contacted and back junction device, where both the emitter and the back contact are formed by amorphous/crystalline silicon heterostructure, and the grid-less front surface is passivated by a double layer of amorphous silicon and silicon nitride, which also provides a good anti-reflection coating. We remark that only one metallic mask has been used in the entire fabrication process, demonstrating that the mask-assisted deposition of a-Si:H layer is feasible. With the aid of a PC1D model we have deduced the properties of transport and recombination that affect the photocurrent and we have addressed the way for future improvements. Even if several technological aspects have to be optimized, such as the high value of series resistance that strongly limits the efficiency of the cell, a V_{oc} of 687 mV has been reached that can be considered a good starting point to continue to develop this low-temperature process useful to reduce the PV manufacturing cost.

References

[1] http://sunpowercorp.com, 2007.
[2] http://www.sanyo.co.jp/clean/solar/hit_e/hit.html, 2005.
[3] W. Mulligan, R. Swanson, Proc. of 13th NREL Crystalline Silicon Workshop, Colorado, 2003, p. 30.
[4] D. Rose, O. Koehler, N. Kaminar, B. Mulligan, D. King, Proc. of 4th World Conference Photovoltaic Energy Conversion, 2006, p. 2018.
[5] W.P. Mulligan, M.A. Carandang, M. Dawson, D.M. De Ceuster, C.N. Stone, R.M. Swanson, Proc. of 21st European Photovoltaic Solar Energy Conference, 2006, p. 1301.
[6] R.M. Swanson, Proc. of the 31st IEEE PVSEC, Lake Buena Vista, 2005, p. 889.
[7] A. Kress, O. Breitenstein, S. Glunz, P. Fath, G.P. Willeke, E. Buncher, Sol. Energy Mater. Sol. Cells 65 (2001) 555.
[8] Taguchi, K. Kawamoto, S. Tsuge, T. Baba, H. Sakata, M. Morizane, K. Uchihashi, N. Nakamura, S. Kiyama, O. Oota, Prog. Photovolt. Res. Appl. 8 (2000) 503.
[9] M. Taguchi, A. Terakawa, E. Maruyama, M. Tanaka, Prog. Photovolt. Res. Appl. 3 (2005) 481.
[10] E. Maruyama, A. Terakawa, M. Taguchi, Y. Yoshimine, D. Ide, T. Baba, M. Shima, H. Sakata, M. Tanaka, Proc. of 4th World Conference Photovoltaic Energy Conversion, 2006, p. 1455.
[11] M. Tucci, L. Serenelli, S. De Iuliis, M. Izzi, Thin Solid Films 515 (2007) 7625.
[12] M. Tucci, L. Serenelli, S. De Iuliis, E. Salza, L. Pirozzi, Proc. of 21st European Photovoltaic Solar Energy Conference, 2006, p. 1250.
[13] L. Kreinin, N. Bordin, J. Broder, N. Eisenberg, M. Tucci, E. Talgorn, S. De Iuliis, L. Serenelli, M. Izzi, E. Salza, L. Pirozzi, Proc. of 21st European Photovoltaic Solar Energy Conference, 2006, p. 855.
[14] PC1D version 5.3 P.A. Basore, D.A. Clugston University of New South Wales (1998).
[15] M. Tucci, L. Serenelli, S. De Iuliis, D. Caputo, A. Nascetti, G. de Cesare, Proc. of 21st European Photovoltaic Solar Energy Conference, 2006, p. 902.
[16] M. Tucci, G. de Cesare, J. Non-Cryst. Solids 338 (2004) 663.